RESOLUTIONS OF ANALOG RAINFALL RECORDS
RELATIVE TO CHART SCALES
by
Donald L. Chery, Jr., and Dave G. Beaver

## ABSTRACT

Five rainfall distributions, four 1-in rainfall depths and one 3-in rainfall depth were plotted on charts with five different combinations of time and depth scales. The plotted events were read on an analog-to-digital converter by four different researchers. Each reading of a plotted record was compared with the known simulated rainfall-rate distribution. The correspondence of the rainfall rates read from the charts with the actual rainfall rate distribution is measured by an integral squared error and correlation coefficient. The results showed a general correspondence between error and the chart scale and a strong influence of maximum recorded rate and rate distribution on the error. For the chart scales evaluated, error did not become more directly associated with scale, except when recorded rates were less than about 10 in/hr. Error was directly related to the number of points read in any given trace by the relation $E = 16.3N^{-0.426}$.

## INTRODUCTION

The Southwest Watershed Research Center (SWWRC) in Tucson, Arizona, collects analog recordings from over 200 rain gages placed on two major and on four minor watersheds (Chery and Kagan, 1975; and Hershfield, 1971). The charts on these gages are usually changed weekly. Over 10,000 analog rain gage charts are received in the Tucson office each year for processing by the Data Processing Section.

A single gage usually records between 15 and 100 precipitation events annually. With a conservative estimate of an average of 25 events/gage/yr, the SWWRC Data Processing Section annually converts at least 250,000 analog recordings of precipitation to a digital form for further processing by digital computer programs. Similar analog records are being collected and processed at many other Agricultural Research Service (ARS) locations. The 1976 ARS Watershed inventory listed 538 recording rain gages besides those of SWWRC. Hershfield (1971) reported 101 of these gages were digital recording gages, which leaves 437 more gages with similar analog recordings. Besides ARS, many other agencies and institutions have rain gages making similar analog recordings.

The SWWRC rain gages record on charts with two different depth measuring scales and four different time scales (Chery and Kagan, 1975), which probably encompass most recording scales used in gages operated by other agencies. The weighing rain gages were described in the Field Manual for Research in Agricultural Hydrology (Holtan, 1962).

The sampling of precipitation for these types of gages may have errors introduced at three critical places. First, the sampling properties of an 8-in diameter orifice (50.26 in$^2$), usually 36 in above ground level, as compared with precipitation falling on an area many times more extensive is questionable. Second, error is introduced by the transducer and linkage (usually mechanical) to the recording pen. Third, error is involved in the resolution of the scales on the recorder charts and in converting the analog recording to a digital record.

In this analysis we examine the third source of error by plotting a known sequence of rainfall rates on the same charts used on the field instruments, and analyzing the digital record obtained from these simulated rainfall recordings.

## PROCEDURE

The evaluation was made by selecting a set of rainfall distributions, plotting them on the five chart time-depth scales, converting them from an analog-to-digital record with a chart reader, and then making comparative analyses between the actual plotted rates and the final digitized record.

### TEST RAINFALL DISTRIBUTIONS

Previously, four rainfall-rate distributions were selected for model evaluation (Chery, 1976). The fifth distribution was derived from an event with one of the highest rainfall rates in SWWRC records (June 5, 1960, as recorded by gage P64.034). The distribution rate of these five events is shown in Figure 1. The number associated with each event in Figure 1 identifies the rain gage and date of the storm events used for the test. Location 47 is 15 mi west and Location 64 is 150 mi east of Albuquerque, New Mexico. These watersheds are described in a reference edited by Hobbs (1963).

The authors are Research Hydraulic Engineer, USDA, Agriculture Research Service, Western Region, Southwest Watershed Research Center, 442 E. 7th Street, Tucson, Arizona 85705, and Hydrologic Assistant, University of Arizona, Soils, Water and Engineering Department, Tucson, Arizona.
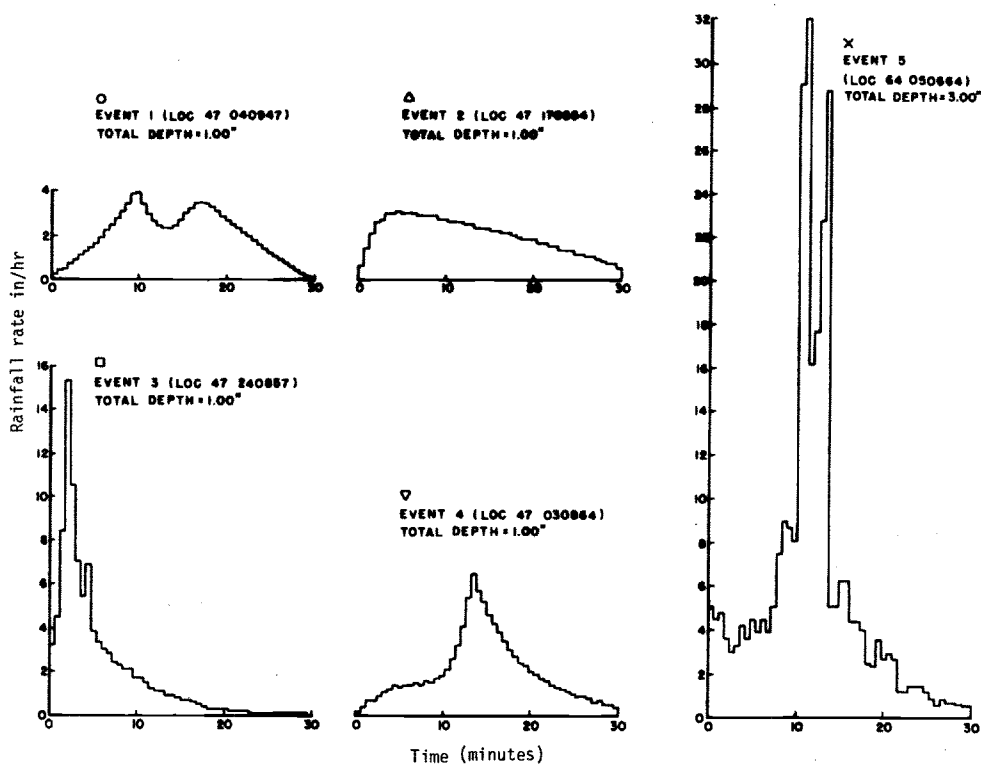
Figure 1.  Rainfall rate distributions for the 5 test events.  Symbols by each event
are used in following figures to identify the indicated event.

The precipitation distributions were plotted at an expanded scale; times and depths were carefully measured, and the distributions were normalized in both time and accumulated depth by dividing by the respective total storm duration and depth.  From the normalized plots, three durations (15, 30, and 90 min) of distributions 1 through 4 were prepared, maintaining a constant 1-in total accumulated depth. For the fifth distribution, the three time distributions (15, 30, and 90 min) were prepared for a 3-in total accumulated depth, which closely matched the measured event.  These events were then read at intervals of 1/50 of the total time, and the rate was computed for each of these intervals.  These rates were then plotted on each of the five different depth-time scale charts.

PLOTTING

The sequence of rates was numerically integrated and the accumulated depth versus time was plotted on field rain gage charts with a Hewlett-Packard[1/] 9125B calculator plotter.  Since the vertical lines on the charts are segments of arcs and the recordings reverse (the recording line goes to the top of the chart and then reverses direction and moves downward on the chart for increasing precipitation depth-- see Holtan (1962) for detailed description of these reversing recording mechanisms), a special program was written to do the plotting.  This program used the relations illustrated in the definition sketch of Figure 2.  With a given time-depth pair (t,d), the program translates the pivotal origin t units, subtracts d from a reference location (Y) of the pivotal origin and calculates the angle $\theta$ as the arcsin (y/r); where y is (Y-d), and r is the pen radius of the rain gage.  The plotting coordinate (x,y) is calculated as (t + rcos$\theta$, Y-d).  The curved vertical axis distorts the recordings of rainfall traces. To test whether this distortion caused differences in the way the same event was read in the analog-to-digital conversion, the same record was plotted at several different positions on the chart.  Plots began at 0, 2.5 and 5 in on the 6-in charts and at 0 and 1 in on the 1.5-in charts.  Figure 3 shows a reproduction of sample plots.

1.  Use of a trade name does not imply endorsement by the U. S. Government but is used for the reader's benefit.
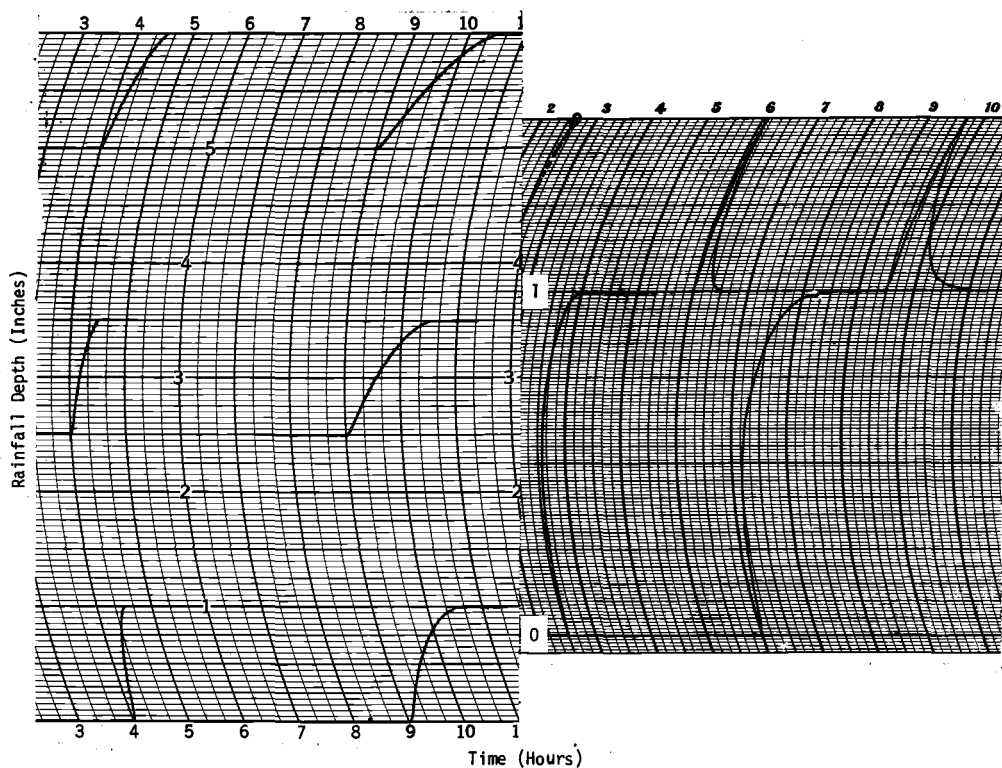
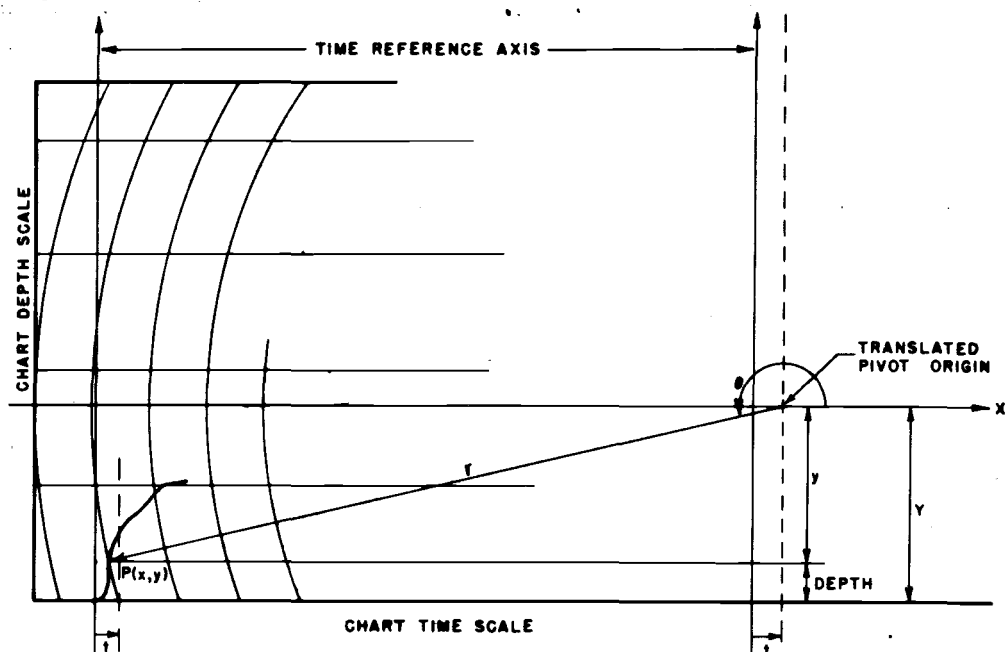Figure 3.  Sample rainfall plots for 6 and 1.5 inch charts with 30 and 90 minute duration events.



Figure 2.  Definition sketch for rainfall plotting program.

217

## DIGITIZATION PROCEDURE

The charts with the simulated rainfall traces were processed by the Southwest Watershed Research Center's normal analog-to-digital conversion process. For a description of this process see Chery and Kagan (1975). The only change in the usual procedure was that we requested that each record be read by several persons. Each chart was read by four persons, except for the weekly charts, which were read manually by one person. The reading of the chart was done by trained operators with from 3-months to 6-yr experience in chart processing.

The analog-to-digital conversion was done by a Benson Lehner[2] Oscar F coupled with a Model F decimal converter. These machines and their operational procedures were described by Osborn (1963).

## ANALYSIS OF DATA

The readings of the simulated charts produced rates that grouped about the actual rates (Figure 4). To evaluate these deviations, an integral squared error (E), as defined by March and Eagleson (1965), and a conventional correlation coefficient ($\rho$) between the read rates ($r_r$) and the actual rates ($r_a$) were calculated for all the readings of each plotted simulated rain rate distribution. These statistics are defined by the following equations:

$$E = \frac{\left[\Sigma \ (r_a - r_r)^2 \right]^{1/2}}{\Sigma r_a} \ X \ 100$$

$$\rho = \frac{n\Sigma r_a r_r - \Sigma r_a \Sigma r_r}{\left[ \{n\Sigma r_a^2 - (\Sigma r_a)^2\} \ \{ n\Sigma r_r^2 - (\Sigma r_r)^2\} \right]^{1/2}}$$

Where n is the maximum count of $r_a$ or $r_r$ used in the period for which comparison is made. These statistics were calculated for each of the different event positions, each different time interval, and each chart type as a whole (all events included).

## RESULTS AND DISCUSSION

The results of the integral squared error and correlation coefficient calculations are listed in Table 1. To evaluate these measurements of error with respect to time and depth scales of the charts, an initial chart resolution parameter was calculated as the inverse of the product of the depth scale (inches of rain/inch of chart) and time scale (min/in of chart), normalized with respect to the smallest value. This parameter was intuitively thought to represent the influence of chart scale on accuracy. The calculation of the resolution parameter was done so that an increasing number would be associated with increasing resolution. The chart scales and calculated resolution parameters are given in Table 2.

Table 2. Chart scales and resolution parameters.

| ID No. | CHART Time per Revolution(T) (hr) | Depth per Traverse(D) (in) | Time Scale (min/in) | Depth Scale (in/in) | Chart Resolution Parameter 1 | Depth Factor | Chart Resolution Parameter 2 |
|---|---|---|---|---|---|---|---|
| 1 | 192 | 6 | 1001.76 | 1.00 | 1 | 1 | 1 |
| 2 | 24 | 6 | 125.22 | 1.00 | 8 | 1 | 8 |
| 3 | 12 | 6 | 62.61 | 1.00 | 16 | 1 | 16 |
| 4 | 24 | 1.5 | 125.22 | 0.333 | 24 | 1.5 | 12 |
| 5 | 6 | 1.5 | 31.30 | 0.333 | 96 | 1.5 | 48 |

As plots of error versus resolution parameter 1 were prepared, it became evident that chart number 4 had errors greater than did chart number 3 as shown in Figure 5. Resolution parameter 1 was apparently not a good index of the information that could be obtained from a chart. The number of points that could be read on any given trace is a function of the time scale of the chart. The comparison of errors

2. Use of a trade name does not imply endorsement by the U. S. Government but is used for the reader's benefit.
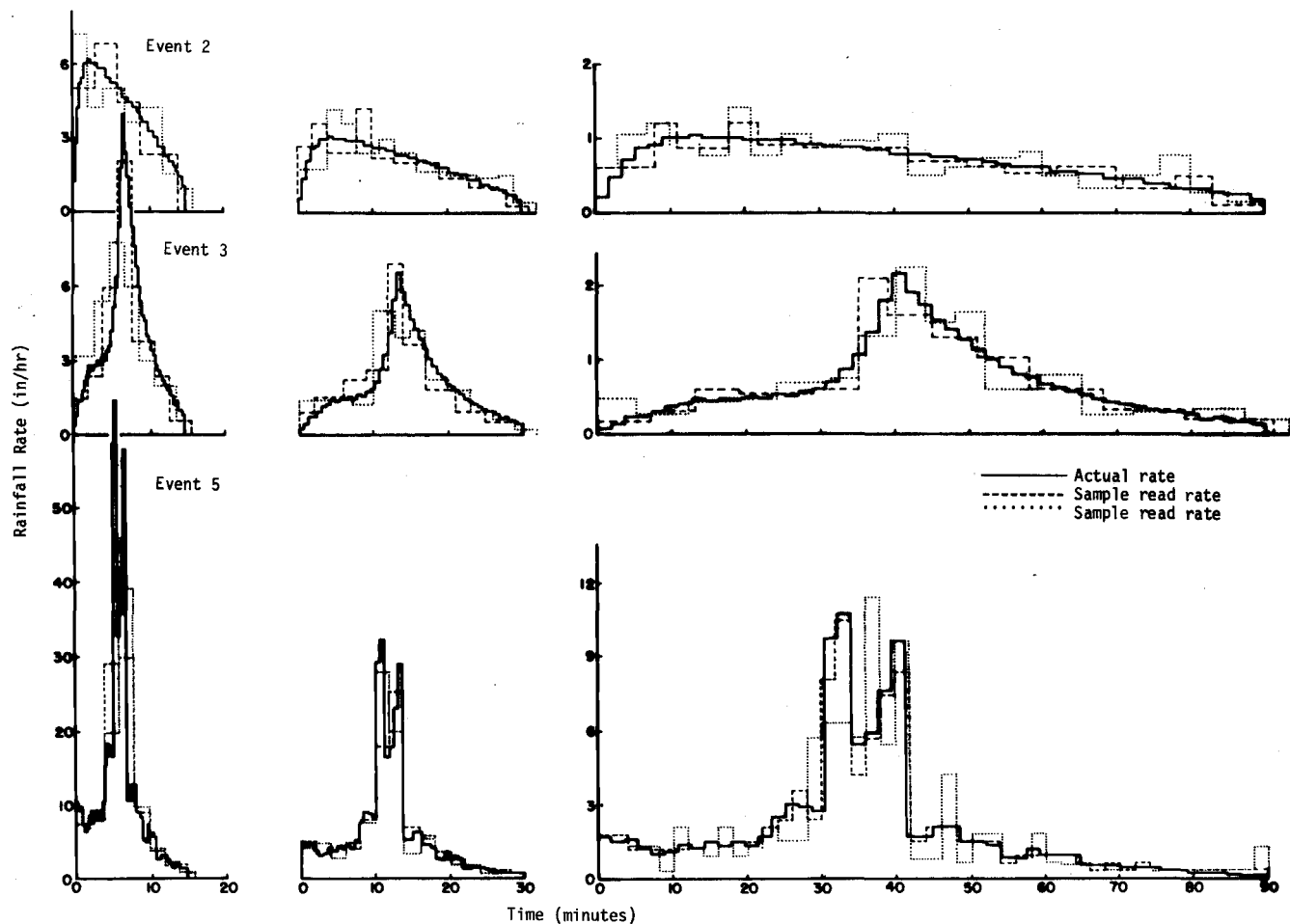
Figure 4. Selected read rainfall rates versus actual rainfall rates for events 2, 3, and 5, at the three event durations of 15, 30 and 90 minutes.

Table 1. Integral Squared Error (E) and Correlation Coefficient (ρ) Values for the Indicated Rain Gage Chart and Simulated Rainfall Event.

| Chart T D | Event No's | Dur | r_m | E Trace Ave. | E Total Chart Ave. | ρ Trace Ave. | ρ Total Chart Ave. | Chart T D | Event No's | Dur | E Trace Ave. | E Total Chart Ave. | ρ Trace Ave. | ρ Total Chart Ave. |
|---|---|---|---|---|---|---|---|---|---|---|---|---|---|---|
| 6/1.5 | 1 | 15 | 7.92 | 3.15 | | 0.925 | | 12/6.0 | 3 | 15 | 12.48 | | 0.828 | |
| | | 30 | 3.96 | 2.80 | | 0.931 | | | | 30 | 11.81 | | 0.834 | |
| | | 90 | 1.32 | 3.72 | 3.23 | 0.887 | 0.914 | | | 90 | 6.47 | 10.50 | 0.953 | 0.869 |
| | 2 | 15 | 6.00 | 3.34 | | 0.842 | | | 4 | 15 | 7.02 | | 0.808 | |
| | | 30 | 3.00 | 2.37 | | 0.903 | | | | 30 | 5.58 | | 0.868 | |
| | | 90 | 1.00 | 3.10 | 2.94 | 0.869 | 0.871 | | | 90 | 3.95 | 5.52 | 0.933 | 0.870 |
| | 3 | 15 | 30.60 | 10.73 | | 0.799 | | | 5 | 15 | 44.28 | | 0.663 | |
| | | 30 | 15.30 | 10.50 | | 0.882 | | | | 30 | 49.75 | | 0.839 | |
| | | 90 | 5.10 | 4.99 | 10.04 | 0.968 | 0.866 | | | 90 | 45.77 | 46.81 | 0.918 | 0.820 |
| | 4 | 15 | 13.00 | 4.72 | | 0.901 | | | 5 | 15 | 41.90 | | 0.722 | |
| | | 30 | 6.50 | 3.08 | | 0.957 | | | | 30 | 42.17 | | 0.749 | |
| | | 90 | 2.17 | 3.52 | 3.77 | 0.945 | 0.934 | | | 90 | 44.04 | 42.70 | 0.851 | 0.774 |
| | 5 | 15 | 64.20 | 41.78 | | 0.689 | | 24/6.0 | 1 | 15 | 5.97 | | 0.711 | |
| | | 30 | 32.10 | 41.89 | | 0.924 | | | | 30 | 5.50 | | 0.769 | |
| | | 90 | 10.70 | 42.97 | 42.22 | 0.944 | 0.854 | | | 90 | 3.35 | 4.91 | 0.893 | 0.798 |
| | 5 | 15 | 64.20 | 41.90 | | 0.686 | | | 2 | 15 | 5.38 | | 0.758 | |
| | | 30 | 32.10 | 42.17 | | 0.918 | | | | 30 | 4.07 | | 0.796 | |
| | | 90 | 10.70 | 44.04 | 42.70 | 0.915 | 0.840 | | | 90 | 3.17 | 4.22 | 0.840 | 0.798 |
| 24/1.5 | 1 | 15 | | 6.54 | | 0.591 | | | 3 | 15 | 13.32 | | 0.816 | |
| | | 30 | | 4.32 | | 0.839 | | | | 30 | 12.86 | | 0.818 | |
| | | 90 | | 3.40 | 4.75 | 0.906 | 0.779 | | | 90 | 5.49 | 10.85 | 0.965 | 0.860 |
| | 2 | 15 | | 5.75 | | 0.546 | | | 4 | 15 | 7.14 | | 0.766 | |
| | | 30 | | 4.50 | | 0.798 | | | | 30 | 6.18 | | 0.817 | |
| | | 90 | | 3.11 | 4.39 | 0.874 | 0.734 | | | 90 | 4.11 | 5.66 | 0.925 | 0.844 |
| | 3 | 15 | | 14.15 | | 0.816 | | | 5 | 15 | 41.06 | | 0.104 | |
| | | 30 | | 11.62 | | 0.817 | | | | 30 | 47.90 | | -0.010 | |
| | | 90 | | 9.96 | 12.90 | 0.876 | 0.786 | | | 90 | 43.41 | 44.12 | -0.034 | .0198 |
| | 4 | 15 | | 10.02 | | 0.597 | | 196/6.0 | 1 | 15 | 7.87 | | 0.057 | |
| | | 30 | | 6.61 | | 0.787 | | | | 30 | 10.03 | | 0.163 | |
| | | 90 | | 4.74 | 7.13 | 0.889 | 0.758 | | | 60 | 8.00 | | 0.202 | |
| | 5 | 15 | | 46.42 | | 0.172 | | | | 90 | 7.19 | 8.27 | 0.431 | 0.213 |
| | | 30 | | 46.34 | | 0.423 | | | 2 | 30 | 6.30 | | 0.728 | |
| | | 90 | | 40.98 | 44.58 | 0.891 | 0.496 | | | 60 | 5.33 | | 0.687 | |
| 12/6.0 | 1 | 15 | | 5.48 | | 0.770 | | | | 90 | 5.45 | 5.69 | 0.311 | 0.575 |
| | | 30 | | 4.46 | | 0.834 | | | 3 | 30 | 17.43 | | 0.585 | |
| | | 90 | | 3.67 | 4.54 | 0.884 | 0.829 | | | 60 | 17.22 | | 0.586 | |
| | 2 | 15 | | 4.62 | | 0.777 | | | | 90 | 15.34 | 16.67 | 0.728 | 0.633 |
| | | 30 | | 3.72 | | 0.812 | | | 4 | 30 | 10.56 | | 0.144 | |
| | | 90 | | 3.12 | 3.86 | 0.841 | 0.808 | | | 60 | 10.55 | | 0.151 | |
| | | | | | | | | | | 90 | 12.00 | 11.04 | 0.214 | 0.027 |

for charts 3 and 4 (Fig. 5) indicated that chart resolution was not improved by tripling the depth-measuring sensitivity if the time scale is decreased by half. The net effect of the disproportionate scale is greater error as shown in Figure 5 and Table 1. Thus, a reordering of the resolution parameter by redefining the influence of the depth scale. Instead of weighting the 0.333 in/in depth scale as 3, we arbitrarily weighted it as 1.5 and calculated another set of chart statistics (resolution parameter 2), as listed in Table 2.

This revised hierarchy of ranking the charts is supported by the descending order of average number of points read from 15-, 30-, and 90-min traces versus resolution parameter 2 (Figure 6).

The results of all the integral squared errors and correlation coefficients are plotted in Figure 7. The upper row of plots are correlation coefficients and the lower row are integral squared errors. All plots show a general tendency (as shown by the encompassing envelope lines -- points for the unusual number 5 event excluded in the integral squared error plots) for increasing errors (correlation coefficient decrease) as resolution parameter 2 decreases. This tendency is more pronounced in the short-duration events. The more pronounced error in the 15-min duration plots is associated with the limited number of points that can be read from a trace of that duration, and will be more fully discussed later in the discussion.

There are still situations (Figure 7A, B, D, and E) where greater errors were obtained from chart number 4 than would be expected by its ranking. This situation may result from less operator experience with this type of chart (only 38 gages of over 200 gages regularly processed) but, probably more importantly, it may be due to the disproportion between the depth and the time scales. The depth scale has the most resolution (0.333 in/in of rain/in of chart) and the time scale has the lowest (125.22 min/in) aside from the weekly charts. The consequence of this disporportion is that the rates obtained from the reading process fluctuate more widely about the actual rates, and thus produce a greater error value.
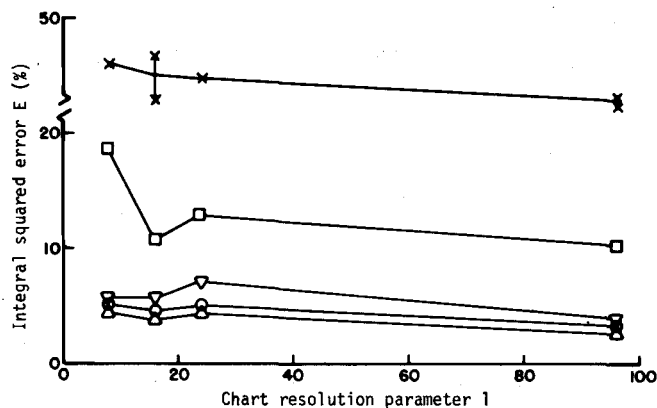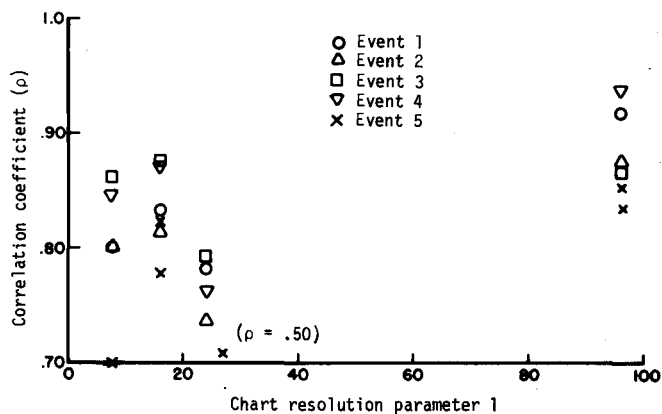
220

Figure 5. Chart resolution parameter number 1 versus integral squared error (E) and correlation coefficient (ρ).
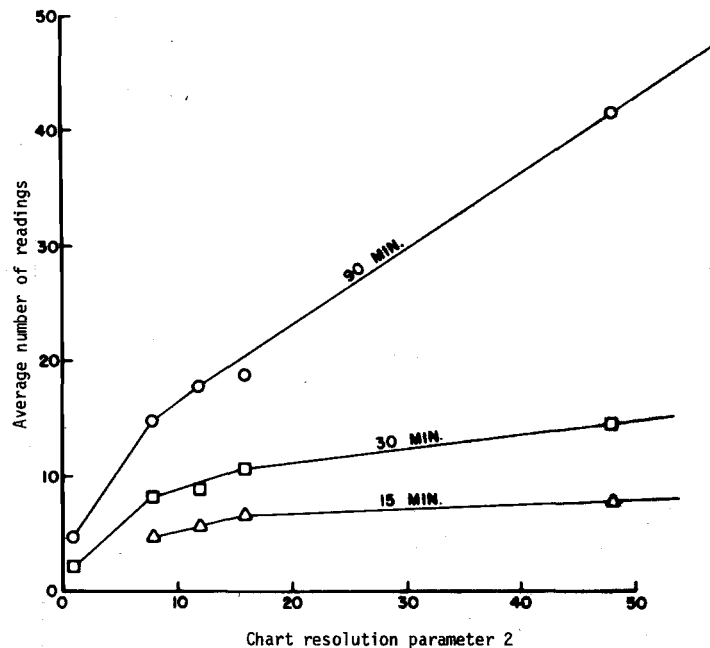


Figure 6. Average number of readings per event versus chart resolution parameter 2.
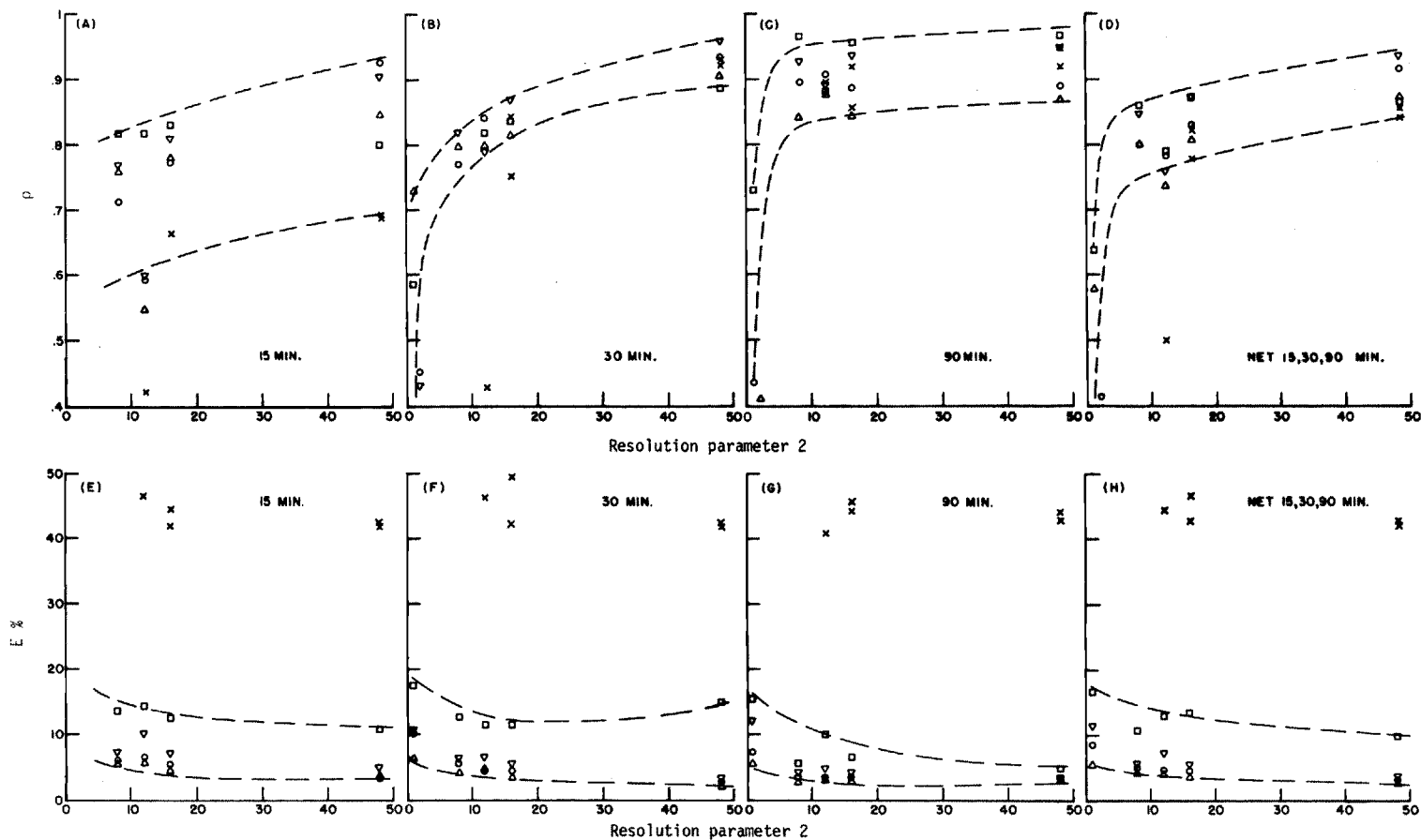
Figure 7.   Mean integral squared error (E) and mean correlation coefficient (ρ) versus chart resolution parameter 2 for all events.

The magnitude of the rates and distributions of high rates in a recorded event affect the error in the reading of the events. The correlation coefficient only reflected the influence of high rates on error in the short (15 min) duration event. The integral squared error consistently reflected the influence of rainfall rate. Event number 5, with the highest maximum rainfall rate, consistently had the highest E values. Event number 3, with the second highest maximum rate, was consistently second highest in integral squared error. The correlation coefficient showed correlation decreased as the chart scale resolution decreased.

The direct relation of error to maximum rainfall rate for the 15- and 30-min duration events is illustrated in Figure 8. Though not indicated on Figure 8, the 15-min duration points distinctly arranged
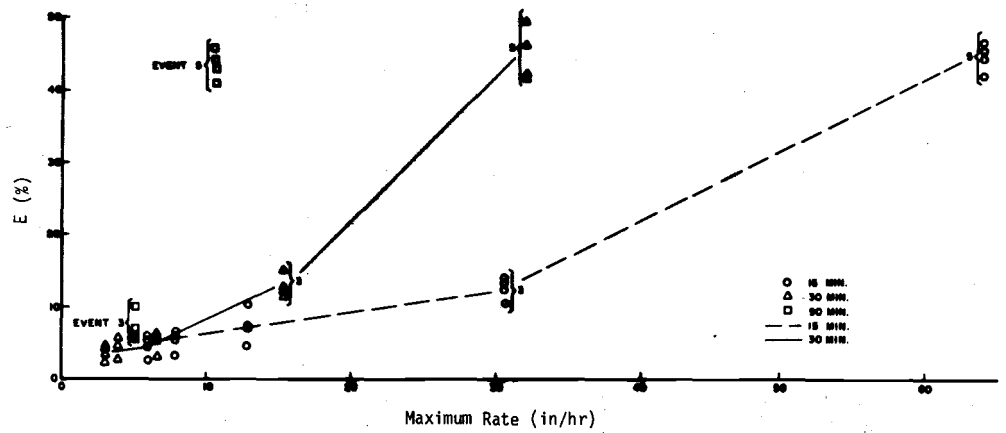


Figure 8. Integral squared error (E) versus maximum rainfall rate for the 15 and 30 minute durations of all 5 test events.

themselves according to chart. Chart 5 (48) (chart resolution parameter 2 is in parenthesis beside each chart identification number) had the lowest error and then in ascending order by error were charts 3 (16), 2(8), and 4(12). However, the error is not uniquely related to maximum rate. In Figure 8, one can see that for similar distribution of rates (event 5) the maximum rate can be from 64.2 to 32.1 to 10.7 in/hr with the integral squared error remaining the same, between 40 and 50 percent. Another event with a high maximum rate (event 3) demonstrates this same performance. As the maximum rate is decreased from 30.6 to 15.3 in/hr, the error for the entire event remained similar, between 10.5 and 15 percent. Not until the maximum rates for event 3 decreased to 5.1 in/hr did the error significatly decrease, although it was still higher than the error for event 2 with a slightly higher peak rate of 6 in/hr.

Evidently, error is associated not only with the maximum rate of input recorded on the chart, but also with the distribution of the rates. By comparing the higher error of the 30 min event 5 with that of the 15 min event 3 (both had nearly the same maximum rate) and the 90 min event 3 with the 30 min event 2, we can infer that increased frequency of input rates (size and number of rate distribution peaks) is associated with increased error.

In essence, the amount of error is associated with the number of points that can be measured on a recorder trace. Obviously, for a chart with a given time scale, there is a limited number of points that can be read to describe an event (see Fig. 6). Associated with the number of points that can be read for a given duration is the minimum length of time into which the recording can be resolved. Table 3 lists the mean number of readings for each chart type and event duration, as well as the time interval that would elapse between readings if the readings were evenly spaced. This table indicates the tendency of chart-readers to increase the average duration between points as the length of the recorder trace increased for charts 1 and 4, a tendency which might explain the variation in $\sigma_n$ with event length. This tendency could be described as an operator bias. Where a definite procedural policy requires a reading every 2 min, as in the processing of chart 5, only slight increases (from 1.91 to 2.07 to 2.17 min duration) were observed.

Obviously, the chart scales were too gross to record with any fidelity the complexities and high rates of event 5. Excluding event 5 from the group of events, an average of the integral squared errors for all the remaining events was calculated and plotted versus the number of points read (Fig. 9). There was a definite power relation between the error and number of points read, which we calculated as

$$E = 16.3N^{-0.426}$$

with $\rho = -.934$

where E is the integral squared error

N is the number of points read.

223

Table 3. Time and depth intervals associated with average number of readings obtained for each type of chart.

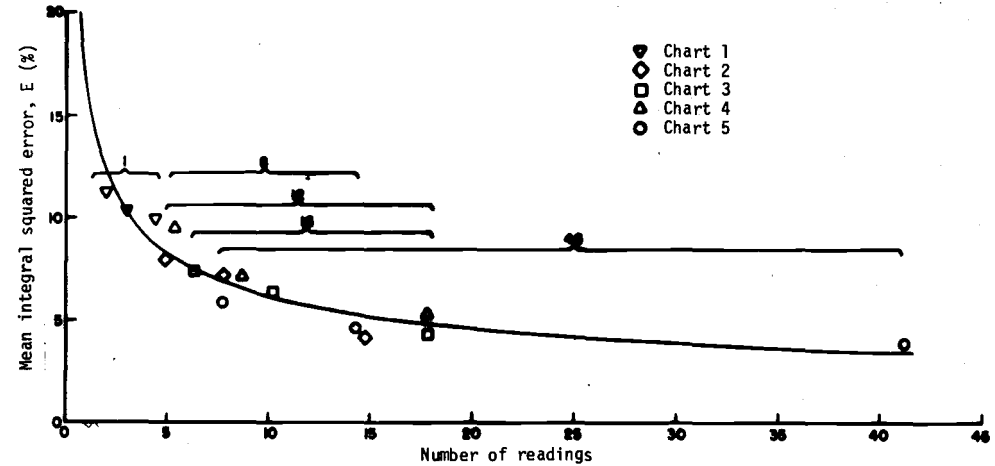| | Chart ID | | Event Duration | | | | | | | | |
|---|---|---|---|---|---|---|---|---|---|---|---|
| | | | 15 min | | | 30 min | | | 90 min | | |
| No. | T/D | R.P. | Number of Intervals | $\sigma_n$ | Time Interval | Number of Intervals | $\sigma_n$ | Time Interval | Number of Intervals | $\sigma_n$ | Time Interval |
| 1 | 192/6 | (1) | | | | 2.0 | 0.0 | 15.0 | 4.5 | 1.56 | 20.0 |
| 2 | 24/6 | (8) | 4.84 | 1.10 | 3.13 | 7.80 | 1.60 | 3.74 | 14.76 | 3.62 | 6.11 |
| 3 | 12/6 | (16) | 6.44 | 1.53 | 2.30 | 10.21 | 2.14 | 2.86 | 17.89 | 5.98 | 4.77 |
| 4 | 24/15 | (12) | 5.43 | 1.00 | 2.74 | 8.70 | 1.49 | 3.40 | 17.74 | 3.92 | 5.10 |
| 5 | 6/15 | (48) | 7.81 | 0.59 | 1.91 | 14.38 | 1.13 | 2.07 | 41.36 | 5.71 | 2.17 |



Figure 9. Mean integral squared error versus the number of readings for events 1-4 at 15, 30, and 90 minute durations.

The span of points in the plots again grouped themselves in the same hierarchy as calculated by resolution parameter 2. Chart number 3 (resolution parameter 2 = 16) had the same number of readings in 90 min as chart number 4 (resolution parameter 2 = 12), which indicated that on the longer duration events, chart number 3 was not read as well as it possibly could have been.

The plot of Figure 9 also indicates a drastic decrease in error improvement, after more than 20 points are read. This leveling-off of the error may indicate that there is an average threshold of error beyond which not much improvement can be expected. Figure 4 indicates that there is a tendency to underread the high peak rates and overread the lower ones, and to oscillate about the real rate on the rises and recessions of the distributions. This oscillation about the real rates always contributes to some value of error, which Figure 9 shows will be between 4 and 5 percent (for the net of four rainfall distributions excluding the unusual event 5 distribution).

That the error in reading any trace is associated with the number of points read is evidence similar to that found by Chery and Lane (1972) in evaluating methods of calculating flow into ponds. Those evaluations showed "that at least 20 divisions per event should be taken to assure that the error will not be greater than -1 percent" (Chery and Lane, 1972, p 435).

## CONCLUSIONS

Error can be associated with chart scale combinations, but more importantly, greater error will be associated with both the peak values and distribution of high rates. Not until peak rainfall rates fall below about 10.0 in/hr does error become principally associated with chart scales.

Also important is the association of error with the number of points read. If the duration of an event and the chart scale are known, a minimum number of points could be specified that would produce an acceptable level of error. Such limits on the number of points could be checked by a precipitation-data checking program that would note readings falling below a specified limit. This information may also be useful in establishing operational procedures on other types of analog-to-digital conversion equipment, in which points can be read at preset frequencies, as the cursor is moved along the analog trace on the chart.

Chart 4 has a poor proportion between depth and time scales. When possible, this situation could be improved by changing the time scale of these gages from 24 hr/revolution to 12 or 6 hr/revolution, or by replacing the gage with a 6 in-24 hour gage.

## REFERENCES CITED

Chery, D. L. 1976. An approach to the simplification of watershed models for applications purposes. Ph.D. dissertation, Utah State University, Logan, Utah.

Chery, D. L. and Kagan, R. S. 1975. An overview of the precipitation processing system at the Southwest Watershed Research Center. National Symposium on Precipitation Analysis for Hydrologic Modeling. Precipitation Committee. Section of Hydrology. AGU. Davis, California. pp 48-59. June 26-28.

Chery, D. L., Jr. and Lane, L. J. 1972. Calculation of pond inflow hydrographs by a chord slope method and a volume increment method. Trans. ASAE, 15(3):433-435 and 439.

Hershfield, D. M. 1971. Agricultural Research Service precipitation facilities and related studies. ARS 41-176.

Hobbs, H. W. 1963. Hydrologic data for experimental agricultural watersheds in the United States. 1956-59. Misc. Pub. No. 945. USDA. Agricultural Research Service. November.

Holtan, H. N., Minshall, N. E., and Harrold, L. L. 1962. Field manual for research in agricultural hydrology. Agriculture Handbook No. 224. USDA. Agriculture Research Service.

March, F., and Eagleson, P. S. 1965. Approaches to the linear synthesis of urban runoff systems. Hydrodynamics Laboratory Report No. 85 (Revised), M.I.T. Cambridge, Mass. September.

Osborn, H. B. 1963. Use of chart readers for analog-to-digital conversion of hydrologic data. USDA. ARS 41-81, 11 pages.